


## RESEARCH ARTICLE

# A quasi-solid polymer electrolyte-based structural battery with high mechanical and electrochemical performance

Gerald Singer<sup>1</sup> | Cheng-Tien Hsieh<sup>2</sup> | Tianwei Jin<sup>1</sup> | Seung Hoon Lee<sup>3</sup> | Yuan Yang<sup>1</sup> 

<sup>1</sup>Program of Materials Science and Engineering, Department of Applied Physics and Applied Mathematics, Columbia University, New York, New York, USA

<sup>2</sup>Department of Chemical Engineering, Columbia University, New York, New York, USA

<sup>3</sup>Department of Mechanical Engineering, Columbia University, New York, New York, USA

## Correspondence

Yuan Yang, Program of Materials Science and Engineering, Department of Applied Physics and Applied Mathematics, Columbia University, New York, NY 10027, USA.

Email: [yy2664@columbia.edu](mailto:yy2664@columbia.edu)

## Funding information

Air Force Office of Scientific Research, Grant/Award Numbers: FA9550-20-1-0233, FA9550-22-1-0226; Austrian Science Fund, Grant/Award Number: J-4476-N

## Abstract

Structural batteries are attractive for weight reduction in electric transportation. For their practical applications excellent mechanical properties and electrochemical performance are required simultaneously, which remains a grand challenge. In this study, we present a new scalable and low-cost design, which uses a quasi-solid polymer electrolyte (QSPE) to achieve both remarkably improved flexural properties and attractive energy density. The QSPE has a high ionic conductivity of  $1.2 \text{ mS cm}^{-1}$  and retains 91% capacity over 500 cycles in graphite/NMC532 cells. Moreover, the resulting structural batteries achieved a modulus of 21.7 GPa and a specific energy of  $127 \text{ Wh kg}^{-1}$  based on the total cell weight, which to our knowledge is the highest reported value above 15 GPa. We further demonstrate the application of such structural batteries in a model electric car. The presented design concept enables the industrialization of structural batteries in electric transportation and further applications to improve energy efficiency and multifunctionality.

## KEYWORDS

electric transportation, multifunctional composites, power hood, quasi-solid polymer electrolyte (QSPE), structural battery

## 1 | INTRODUCTION

Lithium-ion batteries (LIBs) are promising solutions to advance electrified transportation in electric vehicles and electric airplanes. Energy density is one of the most critical parameters for such mobile applications.<sup>1</sup> State-of-the-art commercial LIBs with Ni-rich cathodes reach a specific energy of  $250\text{--}300 \text{ Wh kg}^{-1}$ ,<sup>2</sup> and new innovations in battery materials are pushing even further towards  $400 \text{ Wh kg}^{-1}$  and beyond.<sup>3</sup> However, batteries with high energy density raise safety concerns due to the risk of thermal runaway,<sup>4</sup> or leakage of flammable liquids under

mechanical abuse.<sup>5</sup> To prevent mechanical damage, protective components are usually required to reach safety requirements for certain applications,<sup>6</sup> which adds additional weight to the system and reduces the overall energy density.

The concept of “structural batteries” introduced mechanical reinforcements to batteries to create multifunctional materials that are capable of energy storage and load bearing concurrently. Therefore, the increase of overall energy storage capacity and weight reduction are achieved simultaneously.<sup>7</sup> The total weight of a structural battery is lower than the sum of comparable monofunctional

This is an open access article under the terms of the [Creative Commons Attribution](https://creativecommons.org/licenses/by/4.0/) License, which permits use, distribution and reproduction in any medium, provided the original work is properly cited.

© 2023 The Authors. *EcoMat* published by The Hong Kong Polytechnic University and John Wiley & Sons Australia, Ltd.

structural and energy storage components that fulfill the same functions (i.e., separate carbon fiber composite + battery). This can be expressed as a multifunctional efficiency coefficient  $\eta > 1$ , which is the sum of energy density and mechanical properties normalized to their corresponding benchmarks.<sup>8</sup> Therefore, structural batteries are considered as promising candidates for applications in aviation, automotive, marine, spacecraft and consumer electronics,<sup>7a</sup> and even in robotics.<sup>9</sup>

The characteristics of a structural battery under bending stress are important criteria for their practical applications such as airplane wings and car roofs.<sup>10</sup> However, flexural properties are often the weakest among different types of mechanical stress (e.g., compression and stretching). This issue arises from the fact that external load cannot be effectively transferred between thin layered components inside a battery (e.g., electrode sheets, separators), since they are not mechanically linked together. Several approaches have been demonstrated to solve this problem, including improving the interfacial adhesion,<sup>11</sup> and utilizing secondary bonding,<sup>12</sup> introducing interlocking rivets to the electrode stack,<sup>13</sup> external strengthening,<sup>14</sup> internal structural electrodes,<sup>15</sup> or replacing the liquid electrolyte by a polymer/gel-based solid electrolyte.<sup>16</sup>

Compared to other methods, replacing liquid electrolytes with polymer/gel-based solid electrolytes is a highly scalable and low-cost approach, since it merely introduces additional steps in the battery manufacturing. All-solid-state electrolytes have been explored for new generations of energy storage devices,<sup>17</sup> and particularly quasi-solid/hybrid composite polymer electrolytes have shown advantages in cycle stability with different battery chemistries.<sup>18</sup> Unfortunately, currently reported polymer/gel electrolytes possess a combination of either high ionic conductivity but low mechanical properties,<sup>19</sup> or high mechanical properties but low ionic

conductivity.<sup>20</sup> Therefore, the reported cells have high mechanical properties but unsatisfactory electrochemical performance, or good electrochemical performance but insufficient mechanical strength. For example, Asp et al.<sup>16</sup> reported a structural battery with a high modulus of 25 GPa with a specific energy of 23.6 Wh kg<sup>-1</sup> based on total weight of the cell. Chang's group achieved 131 Wh kg<sup>-1</sup> including the total cell weight and a flexural modulus of 9.6 GPa by using internal rivets, calculated from the reported data.<sup>13</sup> However, the manufacturing process becomes more complicated. Other studies achieved tensile moduli of 12.8 GPa<sup>21</sup> and 5.7 GPa<sup>22</sup> with specific energy of 181.5 and 159 Wh kg<sup>-1</sup>, respectively, but only masses of active electrode materials are included. Such high specific energies will drop significantly (e.g., 40%–60%) with other components included (e.g., current collectors, separators, electrolyte, and packaging).

In this work, we present a quasi-solid polymer-based electrolyte (QSPE) with attractive structural and electrochemical properties for structural batteries simultaneously. It is composed of trifunctional acrylate monomers and dual-salt electrolyte mix that can be thermally in-situ polymerized at a low temperature of 55°C. The as-polymerized electrolyte has a good ionic conductivity of 1.2 mS cm<sup>-1</sup>, and flexural modulus of 176 MPa and strength of 2.7 MPa. Therefore, it can efficiently transfer load from one layer to another without significantly compromising ion transport (Figure 1A). Moreover, this electrolyte is stable with both NMC532 cathode and graphite anode, as we achieved stable cycling over 500 cycles with a capacity retention of 91%. With such a QSPE and carbon fabric/epoxy composite packaging, we achieved significantly increased flexural modulus of 21.7 GPa and flexural strength of 184 MPa, along with a high specific energy of 127 Wh kg<sup>-1</sup> based on total cell mass. The mechanical properties are much lower

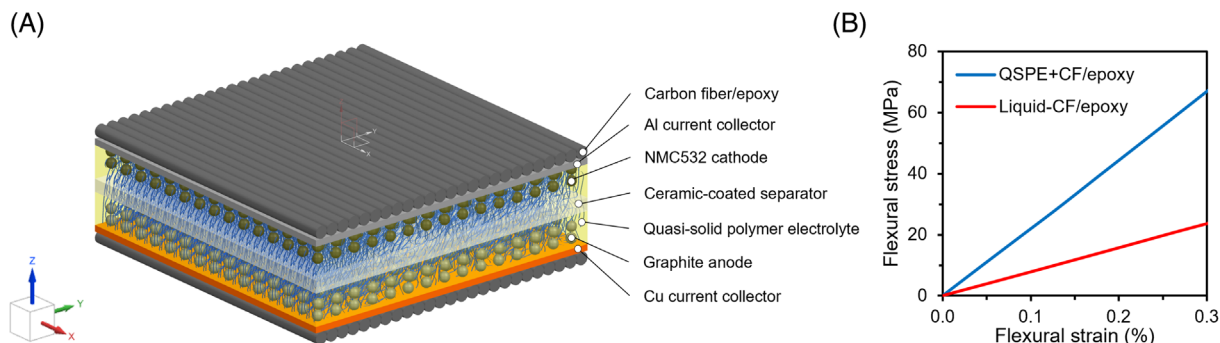


**FIGURE 1** (A) A schematic representation of the structural battery design with internal quasi-solid polymer electrolyte (QSPE) and external carbon fiber (CF)/epoxy composite face sheets for enhancing their mechanical properties. The optimized design provides effective structural integrity of all cell components and excellent electrochemical stability with high energy density. (B) Comparison of finite element simulations of three-point bending tests of structural batteries with a QSPE and a liquid electrolyte. CF fabric/epoxy composite sheets are used as packaging in this simulation.

in identical cells with liquid electrolyte (13.3 GPa and 140 MPa for flexural modulus and strength, respectively).

Moreover, a prototype of a “power hood” was further developed to replace the standard battery and hood of a small model car. The potential practical application of such a structural battery for EVs and their resulting benefits are discussed for three modern EV models, indicating a potential increase of about 10 kWh of “mass-less” energy storage capacity. For an average EV with a 60 kWh battery pack this would increase the capacity by ca. 17% and extend the mileage by an additional 67 km for an energy consumption of 15 kWh/100 km. We believe that the presented design concept represents an important step towards the practical application of structural batteries in the electric transportation industry, for example, electric vehicles (EVs), electric bikes/scooters, drones, airplanes, or in spacecraft technology as well as in portable consumer electronics, such as laptops, tablets, or smartphones.

## 2 | RESULTS

### 2.1 | Mechanical simulations of structural batteries

To understand the effects of the developed polymer electrolyte on the flexural properties of a structural battery, we first performed a quasi-static 2D plane-stress finite element (FE) analysis of a three-point bending test of a Li-ion cell, which has two cell units between carbon fiber (CF) fabric/epoxy composites (Figure 1B). We used a CPS4R shell element, which can capture the bending behavior accurately, as it accounts for the in-plane and out-of-plane deformation without the high computational expense of 3D solid elements. The results show a dramatic increase of the flexural modulus when liquid electrolyte is replaced by the as-developed QSPE. This improvement arises from the ability of the QSPE to transfer mechanical loads between different layers inside a battery, which is not the case when liquid electrolyte is used. Details about the simulation are explained in the supporting information and in Table S1. The corresponding experimental results are discussed and compared with these simulation results in the mechanical properties section.

### 2.2 | Characterizations of the quasi-solid polymer electrolyte

To prepare the QSPE, 1 M lithium difluoro(oxalato) borate (LiDFOB) and 0.4 M lithium tetrafluoroborate

(LiBF<sub>4</sub>) were dissolved in diethyl carbonate and fluoroethylene carbonate (DEC/FEC 2:1 vol) to form a dual-salt electrolyte.<sup>23</sup> Subsequently, 10 wt% of trimethylpropane trimethacrylate (TMPTMA) monomer and 0.1 wt% azobisisobutyronitrile (AIBN) thermal initiator were added to the mixture. After homogenization by magnetic stirring, the QSPE was obtained by in-situ thermal polymerization at 55°C inside a battery.

To analyze the effects of polymerization time, electrochemical impedance spectroscopy and Raman spectroscopy measurements were performed. Figure 2A shows the impedance evolution in a stainless-steel (SS) symmetric coin cell during the in-situ polymerization. Without a separator, the ionic conductivity drops from 2.0 mS cm<sup>-1</sup> at 0 h to 1.85 mS cm<sup>-1</sup> at 4 h and remains stable until 12 h, indicating a completion of the polymerization after ~4 h at 55°C. This also suggests that the polymerization already started before the first measurement during the time that was needed to fabricate a coin cell. The addition of a separator reduces the ionic conductivity by a factor of 4–5, as a result of its nanoporosity. The Raman spectra in Figure 2B confirm that signals of the reactive double bonds (C=C) from the monomer disappear after completion of the polymerization, which means that only very few C=C bonds are left during the cycling in full-cells. Throughout the polymerization process, the mixture also gradually changes its appearance from a transparent liquid to a white wax-like solid (inset Figure 2B), which represents the QSPE that was used in all cell testing of electrochemical and mechanical performance.

The temperature-dependent measurements of ionic conductivity in Figure 2B further show that the QSPE demonstrates a high conductivity of 2.0 mS cm<sup>-1</sup> at 60°C and 1.2 mS cm<sup>-1</sup> at 25°C, respectively. When the QSPE is combined with a separator, the conductivities are 0.53 mS cm<sup>-1</sup> at 60°C and 0.41 mS cm<sup>-1</sup> at 25°C, respectively. Such conductivities are still high enough to achieve good electrochemical performance for LIBs.<sup>7a,24</sup>

The oxidation stability of the polymer electrolyte was evaluated using linear sweep voltammetry (LSV), which indicates that the electrolyte is stable up to ~5.5 V, whereas the oxidation of the liquid electrolyte starts at ~4.7 V (Figure 2B). With the obtained results, it can be concluded that the developed QSPE demonstrates sufficiently high ionic conductivity and good stability to be combined with high-voltage electrodes, such as Ni-rich layered oxide cathode materials (i.e., NMC, NCA).

To examine the cycling stability of the developed QSPE, the critical current density (CCD) was tested in a Li/Li symmetric cell with 1 mAh cm<sup>-2</sup>. Cell failure occurred at the CCD of 12 mA cm<sup>-2</sup> at room temperature (Figure S1), which corresponds to a 4 C rate for standard commercial electrodes with an areal capacity of 3 mAh

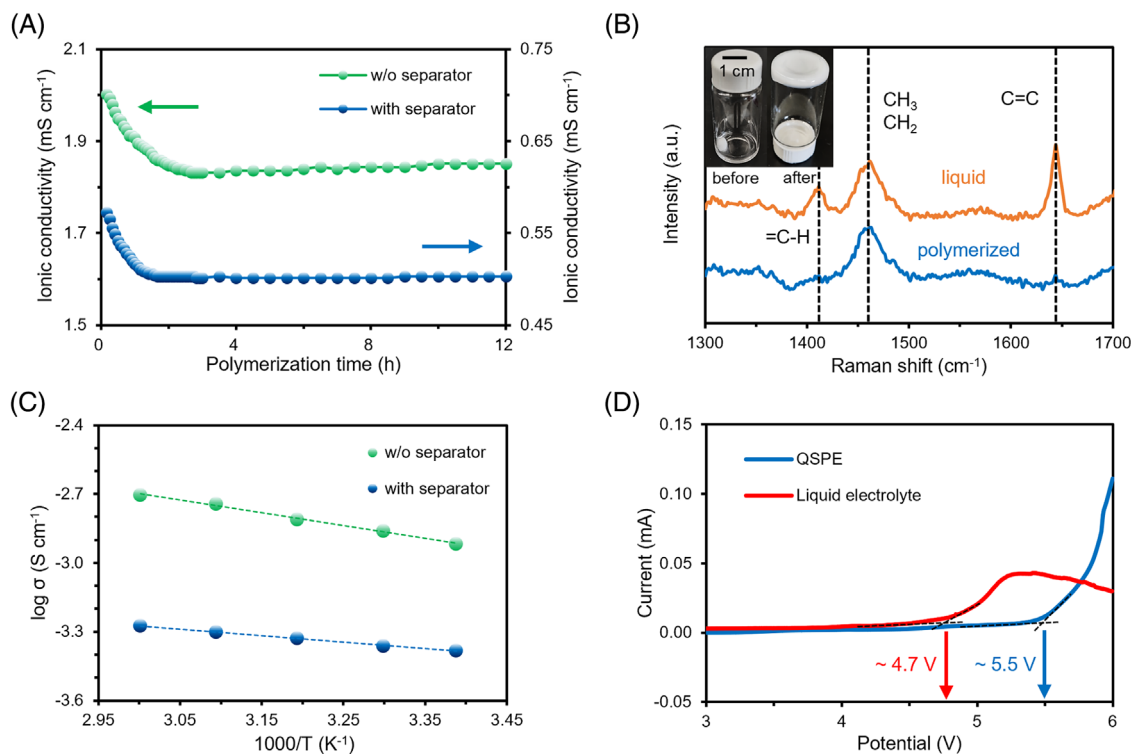


**FIGURE 2** (A) The ionic conductivity of the QSPE with and without separator during the thermal polymerization in a stainless-steel (SS) symmetric coin cell. The results indicate the completion of the reaction after  $\sim 4$  h at  $55^\circ\text{C}$ . (B) Raman spectra of the QSPE before and after polymerization. The relevant Raman peaks associated with C=C bonds ( $1645\text{ cm}^{-1}$ ) and =C-H ( $1410\text{ cm}^{-1}$ ) disappear after polymerization at  $55^\circ\text{C}$ . The inset shows the QSPE before and after polymerization in a glass vial. (C) The temperature dependence of ionic conductivity of the QSPE with and without separator between  $20^\circ\text{C}$  and  $60^\circ\text{C}$  in an SS symmetric coin cell. (D) The linear sweep voltammetry (LSV) measurement of liquid electrolyte (1 M  $\text{LiPF}_6$  in EC/DEC 1:1 vol) and the QSPE between open circuit voltage (OCV) and 6 V versus  $\text{Li}^+/\text{Li}$  in a Li/SS coin cell indicates oxidation stability up to  $\sim 5.5$  V versus  $\text{Li}^+/\text{Li}$  for the QSPE.

$\text{cm}^{-2}$ . This observation confirms that this QSPE is suitable for modern electric vehicles, as typically only a C-rate between 1 C and 2 C is required.

### 2.3 | Electrochemical performance

The basic requirement for any novel electrolyte is that it should not significantly compromise the electrochemical performance of batteries. To validate this, we evaluated the electrochemical performance of the QSPE with long-term cycling tests in half-cells (Li/graphite, Li/NMC532) and graphite/NMC532 full-cells at room temperature, and compared the results with a standard liquid electrolyte consisting of 1 M  $\text{LiPF}_6$  in ethylene carbonate and diethylene carbonate (EC/DEC 1:1 vol).

The Li/NMC532 cells show an initial capacity of  $150\text{ mAh g}^{-1}$  and a capacity retention of 96% after 100 cycles with liquid electrolyte at 0.5 C, and an initial capacity of  $153\text{ mAh g}^{-1}$  and a capacity retention of 91% after 100 cycles with QSPE at 0.5 C (Figure 3A). The lower capacity retention of the QSPE cells may be a result

of slow side reactions between Li metal and the QSPE, especially before full polymerization. The Li/graphite half-cells in Figure 3B show stable cycling in both electrolytes with a good capacity retention of 95% and 93% for QSPE and liquid electrolyte, respectively. The initial capacity during delithiation is  $370\text{ mAh g}^{-1}$  for the liquid electrolyte and  $372\text{ mAh g}^{-1}$  for the QSPE, which is the theoretical capacity of graphite.

We further tested the electrochemical performance of graphite/NMC532 full-cells with a high capacity loading of  $\sim 2.3\text{ mAh cm}^{-2}$ , which is critical for practical applications. The cell demonstrated excellent cycling stability with the QSPE, which resulted in capacity retentions of 95% after 250 cycles and 91% after 500 cycles. In contrast, the capacity retention is only 93% after 250 cycles with the liquid electrolyte (Figure 3C). The long-term cycling life for the QSPE in full-cells was even extended to 1000 cycles with a 1 C charging rate, which showed a high capacity retention of 88% (Figure S3). This further demonstrates the excellent compatibility and stability of the QSPE with both electrodes. We also tested the power capacity of full-cells at different C-rates (Figure 3D).

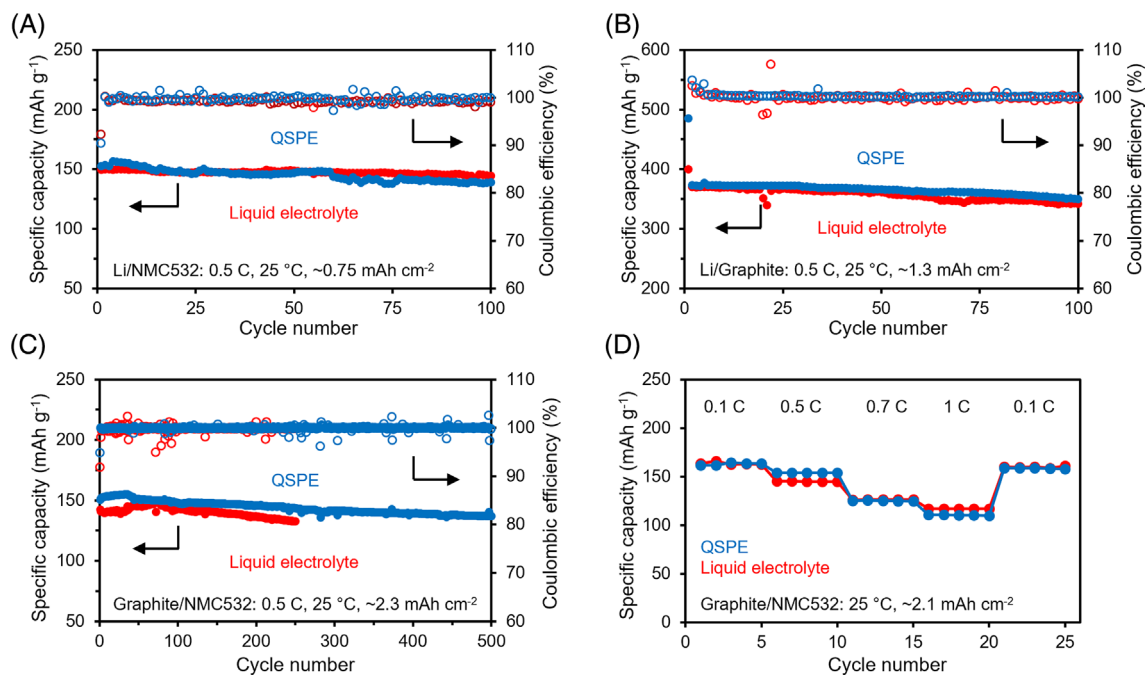


**FIGURE 3** (A–C) Long-term cycling tests at 0.5 C at room temperature of coin cells with liquid electrolyte (1 M LiPF<sub>6</sub> in EC/DEC 1:1 vol) and QSPE. (A) Li/NMC532 and (B) Li/graphite half-cells, and (C) graphite/NMC532 full-cells. (D) C-rate testing of graphite/NMC532 full-cells with QSPE and liquid electrolyte at room temperature.

Comparable specific discharge capacities were observed with both electrolytes. At 0.1 C, 0.5 C and 1 C, the discharge capacities for the QSPE are 163, 154 and 111 mAh g<sup>-1</sup>, respectively. The corresponding values are 163, 145 and 117 mAh g<sup>-1</sup> for the liquid electrolyte.

## 2.4 | Mechanical properties

After validating the electrochemical compatibility of the developed QSPE with electrode materials, we further explored its mechanical properties, and the effects on the flexural properties of pouch cells with three-point bending tests. A schematic of the corresponding cell structure is shown in Figure 4A, where we used two cell units of commercial graphite/NMC532 electrodes with double-sided coating and a capacity loading of 3 mAh cm<sup>-2</sup>. The differences between QSPE and liquid electrolyte are compared in two different packaging materials: conventional plasticized aluminum pouch and carbon fiber fabric/epoxy composite face sheets.

The QSPE itself shows a flexural modulus of 176 MPa with a strength of 2.7 MPa (Figure 4B), which is sufficiently high to transfer mechanical load between the electrodes,<sup>7a</sup> and relatively high compared to similar recently reported polymer electrolytes listed in Table S2. To evaluate the advantages of the QSPE at the cell level, pouch cell-based structural batteries, consisting of

commercial NMC532 and graphite electrodes, separator, electrolyte, and packaging, were assembled, and their flexural properties were measured. The setup is illustrated in Figure S2.

First, cells with conventional plasticized aluminum pouches were tested. Figure 4C shows a dramatic increase in flexural modulus from 0.60 to 4.0 GPa and strength from 4.5 to 13.9 MPa when using the QSPE instead of liquid electrolyte. This can be explained by the strong interfacial adhesion between QSPE and electrodes, therefore, the load can be efficiently transferred from one layer to another. Whereas in the case of the liquid electrolyte the electrodes have no mechanical connection and as a result they easily slide against each other. The performance is also better than in our previous study where we used a tree-root-like interfacial adhesion approach to enhance the flexural modulus, which achieved a flexural modulus of 3.1 GPa.<sup>11a</sup> This is due to the QSPE being much stronger than the porous polyvinylidene fluoride-co-hexafluoropropylene (PVDF-HFP) when it is swollen in liquid electrolyte, which reduces the modulus of PVDF from ~0.6 GPa to ~0.01 GPa.<sup>25</sup>

We further examined the improvement of the mechanical properties in cells with strong carbon fiber fabric/epoxy-based packaging (150–180 μm thick on each side). Such structural batteries were assembled in the same way as described above for pouch cells, except that carbon fiber composites were utilized as structural

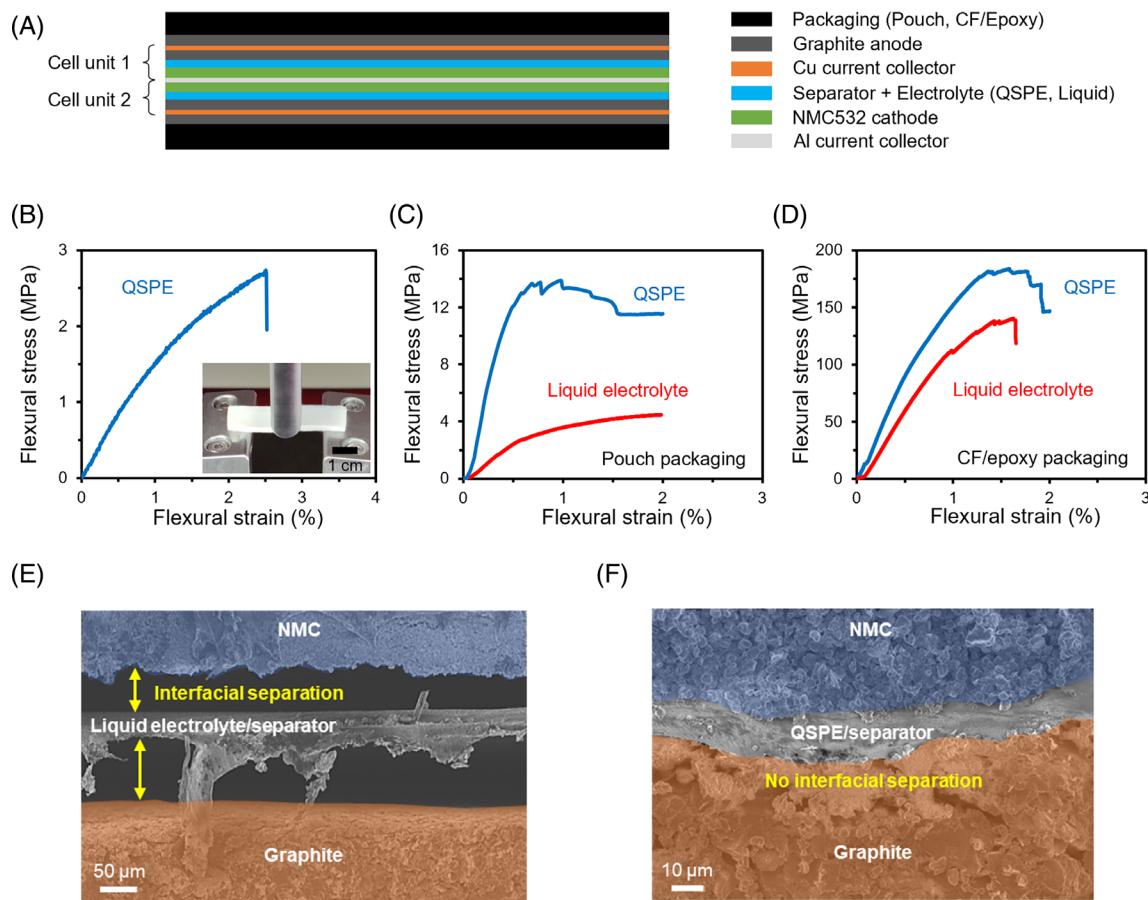


**FIGURE 4** (A) The schematic cell structure for mechanical testing. The packaging is either conventional pouch for Li-ion batteries or carbon fabric/epoxy sheets. Two cell units with double-sided commercial electrodes ( $3 \text{ mAh cm}^{-2}$ ) are used inside a cell. (B) Strain–stress plots from three-point bending tests of the QSPE without a separator. Inset: A QSPE sample during testing. (C/D) Strain–stress curves from three-point bending tests of pouch cells assembled with liquid electrolyte and QSPE in (C) conventional pouches and (D) CF/epoxy face sheets. (E/F) SEM images of the electrode–separator interface on the tension side of the samples with (E) liquid electrolyte showing separation gaps and (F) QSPE without interface separation.

packaging material. The flexural modulus and strength increased from 13.3 to 21.7 GPa and from 140 to 184 MPa, respectively, when replacing the liquid electrolyte with the QSPE (Figure 4D). This means that even with strong CF/epoxy packaging, the introduction of QSPE can still improve the mechanical properties by 30%–70%, since load transfer between layers is important to obtain good flexural properties. These results highlight the importance of structural integrity between different layers in a cell that can be achieved with a mechanically reinforcing electrolyte.

For structural batteries with CF/epoxy packaging, the FE simulation in Figure 1B predicted an elastic modulus of 22.5 GPa using QSPE, which is close to the experimental results (21.7 GPa). For liquid electrolyte, the experiment achieved a higher modulus (13.3 GPa) than the simulated value of 7.9 GPa, which could be due to the additional adhesion at the outside epoxy/electrode interfaces. It should be noted that for simulation

purposes the thickness of the CF/epoxy was fixed at  $180 \mu\text{m}$ , whereas the experimental thickness varied between 150 and  $180 \mu\text{m}$ . A lower thickness could result in a higher flexural modulus than predicted by the model.

To further understand how the QSPE enhances the structural integrity in full-cells, we compared cross-sectional SEM images of the interface on the tension side of structural battery samples with liquid electrolyte (Figure 4E) and QSPE (Figure 4F) after the bending tests were performed. For the sample with liquid electrolyte, large gaps between electrodes and separators were observed due to the lack of physical connection between the layers, in contrast, there was no interfacial separation with the QSPE. Further, the samples with QSPE show only minor signs of interface separation on the compression side (Figure S2c), whereas for liquid electrolyte severe interface separation was present on the compression side (Figure S2d). This observation confirms that the

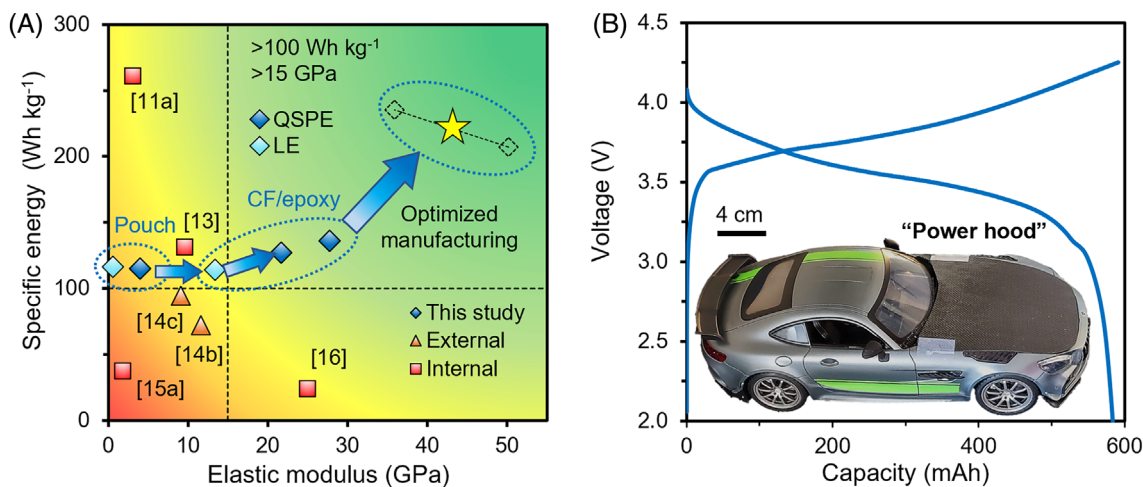


**FIGURE 5** (A) Comparison of the performance metrics of various reported structural batteries. The metrics include the specific energy based on the total cell mass and the elastic modulus of the structural battery. The increase of the elastic modulus due to the replacement of liquid electrolyte (LE) with the QSPE for pouch cells and CF/epoxy sheet underlines the importance of internal reinforcement for mechanical properties. (B) The total capacity of one cell of the structural battery used as a “power hood” for a schematic car model (1:16) to replace the hood of the car.

adhesion between electrodes can be sufficiently enhanced by the QSPE.

## 2.5 | Prototype demonstration

The as-developed structural battery with QSPE has a specific energy of  $127 \text{ Wh kg}^{-1}$  based on the capacity of two cell units of commercial graphite/NMC532 electrodes and the total mass of the battery components including packaging, combined with one of the highest reported elastic moduli in literature, as indicated in Figure 5A. Excluding the outermost two inactive layers of graphite, which are contacting the CF/epoxy packaging, the specific energy can reach  $136 \text{ Wh kg}^{-1}$  and the flexural modulus and strength are 27.7 GPa and 112 MPa, respectively (Figure S3). Such an excellent combination of mechanical and electrochemical performance can be attributed to the optimized design of the developed QSPE.

Based on our estimations, a structural battery assembled under optimized manufacturing conditions can reach a modulus of  $\sim 43 \text{ GPa}$  with a specific energy of  $\sim 220 \text{ Wh kg}^{-1}$  (Figure 5A), assuming CF/epoxy composite with an elastic modulus of  $70 \text{ GPa}$ <sup>26</sup> and lean electrolyte condition ( $3 \text{ g Ah}^{-1}$ ). Different scenarios of modulus and specific energy pairs are shown in Figure S5.

To further demonstrate the potential of the as-developed structural battery, a “power hood” cell was assembled to be integrated with a model car. In this demonstration, the hood of a model car (1:16 scale) was used as the only power source instead of the regular battery pack (Figure 5B, Video S1). The “power hood” was

assembled with two cells in series and 11 repeating cathode/separator/anode units and QSPE in each cell between CF/epoxy face sheets. Each individual cell has a total capacity of ca. 583 mAh (Figure 5B), which exceeds the nominal capacity of 500 mAh in a regular battery equipped with this model car.

The specific energy of the “power hood” reached  $118 \text{ Wh kg}^{-1}$ , compared to  $\sim 68 \text{ Wh kg}^{-1}$ , due to the reduction of weight from 54.3 g (regular hood + original battery) to 36.6 g (structural battery). This corresponds to 13% weight savings and 20% increase in energy storage capacity for the model car. Moreover, the modulus of the original hood was improved by a factor of  $\sim 11$ , from 1.9 to 21.7 GPa (Figure S6). The cycling stability of the QSPE was also demonstrated for 50 cycles of a 900 mAh cell, that was assembled with commercial graphite/NMC532 electrodes with  $3 \text{ mAh cm}^{-2}$  and cycled at 0.3 C under  $30^\circ \text{C}$  (Figure S7).

In practical size EVs, the potential gain of energy storage capacity was calculated using the performance metrics of this as-developed structural battery. Different EV models were compared in Figure S8 regarding their theoretical benefits in storage capacity and weight savings compared to conventional car engineering materials. On average ca. 10 kWh could be added to an EV by replacing inactive car body parts (hood, roof, doors, etc.) with multifunctional structural batteries, adding only a minimal amount of additional weight relative to modern carbon fiber-reinforced plastic (CFRP) parts and substantial weight reduction compared Al or steel parts. For an average EV with a 60 kWh battery pack this would increase the capacity by  $\sim 17\%$  and extend the mileage by 67 km based on an energy consumption of 15 kWh/100 km.

Carlsedt and Asp analyzed the impact of replacing the original battery, interior and exterior components of an EV with structural batteries.<sup>27</sup> For the car model BMW i3, a potential increase of about 70% in the mileage was proposed when a total weight of 615 kg of car components are substituted. However, replacing the original battery and interior car components with structural batteries might be more challenging for manufacturers. In our analysis of the same car model, replacing about 69 kg of exterior car body parts with structural batteries improved the mileage by 19%.

### 3 | CONCLUSION

In this study, we presented a quasi-solid polymer electrolyte (QSPE) with an ionic conductivity of 1.2 mS cm<sup>-1</sup> at room temperature and an oxidation stability of up to 5.5 V versus Li<sup>+</sup>/Li. Graphite/NMC532 full-cells with this QSPE electrolyte also demonstrated a high capacity retention of 91% after 500 cycles at room temperature. The QSPE has sufficiently high modulus and strength to significantly enhance the mechanical properties of structural batteries with either carbon fiber (CF)/epoxy composite face sheets or regular pouches, which stems from its capability to transfer mechanical load between different layers in a battery. For a cell with two units of electrodes and CF/epoxy packaging, the flexural modulus increased from 13.3 GPa with liquid electrolyte to 21.7 GPa with QSPE. Furthermore, due to the good compatibility of the QSPE with electrodes at high mass loadings, the specific energy of structural battery achieved 127 Wh kg<sup>-1</sup> (based on the total cell mass), which to our knowledge is the highest reported in literature with modulus over 15 GPa. We further demonstrate the application of such a structural battery in a model electric vehicle.

Our findings highlight the importance of designing polymer-based electrolytes with good mechanical properties that do not sacrifice electrochemical performance to improve structural batteries in terms of modulus, strength, and energy density. This approach represents an important step towards the industrial application of multifunctional composites as “massless” energy storage in electronic transportation, spacecraft, and further applications.

#### AUTHOR CONTRIBUTIONS

**Gerald Singer:** Concept, experiments, data evaluation and visualization, writing-original draft, funding acquisition. **Cheng-Tien Hsieh:** Experiments. **Tianwei Jin:** Simulation. **Seung Hoon Lee:** Data visualization. **Yuan Yang:** Concept, writing-revision, funding acquisition.

#### ACKNOWLEDGMENTS

Gerald Singer acknowledges the support from the Austrian Science Fund (FWF) [J-4476-N]. The authors acknowledge the support from the Air Force Office of Scientific Research (FA9550-20-1-0233 and FA9550-22-1-0226).

#### CONFLICT OF INTEREST STATEMENT

The authors declare no conflict of interest.

#### ORCID

Yuan Yang  <https://orcid.org/0000-0003-0264-2640>

#### REFERENCES

- a) Wang C-Y, Liu T, Yang X-G, et al. Fast charging of energy-dense lithium-ion batteries. *Nature*. 2022;611(7936):485-490. doi:10.1038/s41586-022-05281-0 b) Li M, Lu J, Chen Z, Amine K. Fast charging of energy-dense lithium-ion batteries. *Adv Mater*. 2018;30:1800561.
- a) Randau S, Weber DA, Kötz O, et al. Benchmarking the performance of all-solid-state lithium batteries. *Nat Energy*. 2020; 5(3):259-270. doi:10.1038/s41560-020-0565-1 b) Choi JU, Voronina N, Sun Y-K, Myung S-T. Recent Progress and perspective of advanced high-energy Co-less Ni-rich cathodes for Li-ion batteries: yesterday, today, and tomorrow. *Adv Energy Mater*. 2020;10(42):2002027. doi:10.1002/aenm.202002027
- a) Liu J, Bao Z, Cui Y, et al. Multiscale polymeric materials for advanced lithium battery applications. *Nat Energy*. 2019;35(4): 180. b) Kang J, Han D-Y, Kim S, Ryu J, Park S. Multiscale polymeric materials for advanced lithium battery applications. *Adv Mater*. 2023;35(4):2203194. doi:10.1002/adma.202203194
- Finegan DP, Darcy E, Keyser M, et al. Characterising thermal runaway within lithium-ion cells by inducing and monitoring internal short circuits. *Energy Environ Sci*. 2017;10(6):1377-1388. doi:10.1039/C7EE00385D
- a) Duan X, Wang H, Jia Y, Wang L, Liu B, Xu J. A multiphysics understanding of internal short circuit mechanisms in lithium-ion batteries upon mechanical stress abuse. *Energy Storage Mater*. 2022;45:667-679. doi:10.1016/j.ensm.2021.12.018 b) Li H, Zhou D, Zhang M, Liu B, Zhang C. Multi-field interpretation of internal short circuit and thermal runaway behavior for lithium-ion batteries under mechanical abuse. *Energy*. 2023; 263:126027. doi:10.1016/j.energy.2022.126027
- Liu K, Liu Y, Lin D, Pei A, Cui Y. Materials for lithium-ion battery safety. *Sci Adv*. 2018;4(6):eaas9820.
- a) Jin T, Singer G, Liang K, Yang Y. Structural batteries: Advances, challenges and perspectives. *Mater Today*. 2022;62: 151-167. doi:10.1016/j.mattod.2022.12.001 b) Galos J, Pattarakunnan K, Best AS, Kyrtzlis IL, Wang C-H, Mouritz AP. Energy storage structural composites with integrated lithium-ion batteries: a review. *Adv Mater Technol*. 2021;6(8):2001059. doi:10.1002/admt.202001059 c) Asp LE, Johansson M, Lindbergh G, Xu J, Zenkert D. Structural battery composites: a review. *Funct Compos Struct*. 2019;1(4):042001. doi:10.1088/2631-6331/ab5571
- O'Brien DJ, Baechle DM, Wetzal ED. Design and performance of multifunctional structural composite capacitors. *J Compos Mater*. 2011;45(26):2797-2809. doi:10.1177/0021998311412207



9. Lutkenhaus JL, Flouda P. Structural batteries take a load off. *Science Robotics*. 2020;5(45):eabd7026. doi:10.1126/scirobotics.abd7026
10. Goodman JKS, Miller JT, Kreuzer S, et al. Lithium-ion cell response to mechanical abuse: three-point bend. *J Energy Storage*. 2020;28:101244. doi:10.1016/j.est.2020.101244
11. a) Jin T, Ma Y, Xiong Z, et al. Bioinspired, tree-root-like interfacial designs for structural batteries with enhanced mechanical properties. *Adv Energy Mater*. 2021;11(25):2100997. doi:10.1002/aenm.202100997 b) Moyer K, Boucherbil NA, Zohair M, Eaves-Rathert J, Pint CL. Polymer reinforced carbon fiber interfaces for high energy density structural lithium-ion batteries. *Sustainable Energy Fuel*. 2020;4(6):2661-2668. doi:10.1039/D0SE00263A
12. a) Kwon SR, Harris J, Zhou T, Loufakis D, Boyd JG, Lutkenhaus JL. Mechanically strong graphene/aramid nanofiber composite electrodes for structural energy and power. *ACS Nano*. 2017;11(7):6682-6690. doi:10.1021/acsnano.7b00790 b) Flouda P, Feng X, Boyd JG, Thomas EL, Lagoudas DC, Lutkenhaus JL. Interfacial engineering of reduced graphene oxide for aramid nanofiber-enabled structural Supercapacitors. *Batteries Supercaps*. 2019;2(5):464-472. doi:10.1002/batt.201800137 c) Flouda P, Yun J, Loufakis D, et al. Structural reduced graphene oxide supercapacitors mechanically enhanced with tannic acid. *Sustainable Energy Fuel*. 2020;4(5):2301. doi:10.1039/C9SE01299K
13. Ladpli P, Nardari R, Kopsaftopoulos F, Chang F-K. Multifunctional energy storage composite structures with embedded lithium-ion batteries. *J Power Sources*. 2019;414:517-529. doi:10.1016/j.jpowsour.2018.12.051
14. a) Thomas JP, Qidwai SM, Pogue WR, Pham GT. Multifunctional structure-battery composites for marine systems. *J Compos Mater*. 2012;47(1):5-26. doi:10.1177/0021998312460262 b) Galos J, Best AS, Mouritz AP. Multifunctional sandwich composites containing embedded lithium-ion polymer batteries under bending loads. *Mater Des*. 2020;185:108228. doi:10.1016/j.matdes.2019.108228 c) Pattarakunna K, Galos J, Das R, Mouritz AP. Tensile properties of multifunctional composites embedded with lithium-ion polymer batteries. *Compos A: Appl Sci Manuf*. 2020;136:105966. doi:10.1016/j.compositesa.2020.105966
15. a) Moyer K, Meng C, Marshall B, et al. Carbon fiber reinforced structural lithium-ion battery composite: multifunctional power integration for CubeSats. *Energy Storage Mater*. 2020;24:676-681. doi:10.1016/j.enstm.2019.08.003 b) Sanchez JS, Xu J, Xia Z, Sun J, Asp LE, Palermo V. Electro-phoretic coating of LiFePO<sub>4</sub>/graphene oxide on carbon fibers as cathode electrodes for structural lithium ion batteries. *Compos Sci Technol*. 2021;208:108768. doi:10.1016/j.compscitech.2021.108768 c) Huang W, Wang P, Liao X, et al. Mechanically-robust structural lithium-sulfur battery with high energy density. *Energy Storage Mater*. 2020;33:416-422. doi:10.1016/j.enstm.2020.08.018
16. Asp LE, Bouton K, Carlstedt D, et al. A structural battery and its multifunctional performance. *Adv Energy Sustainability Res*. 2021;2(3):2000093. doi:10.1002/aesr.202000093
17. Sun C, Liu J, Gong Y, Wilkinson DP, Zhang J. Recent advances in all-solid-state rechargeable lithium batteries. *Nano Energy*. 2017;33:363-386. doi:10.1016/j.nanoen.2017.01.028
18. a) Liu L, Sun C. Flexible quasi-solid-state composite electrolyte membrane derived from a metal-organic framework for lithium-metal batteries. *ChemElectroChem*. 2020;7(3):707-715. doi:10.1002/celec.201902032 b) Qiu G, Sun C. A quasi-solid composite electrolyte with dual salts for dendrite-free lithium metal batteries. *New J Chem*. 2020;44(5):1817-1824. doi:10.1039/C9NJ04897A c) Yi Q, Zhang W, Wang T, Han J, Sun C. A high-performance lithium metal battery with a multilayer hybrid electrolyte. *Energy Environ Mater*. 2023;6:e12289. doi:10.1002/eem2.12289
19. a) Zheng T, Cui X, Chu Y, Li H, Pan Q. Ultrahigh elastic polymer electrolytes for solid-state lithium batteries with robust interfaces. *ACS Appl Mater Interfaces*. 2022;14(4):5932-5939. doi:10.1021/acsami.1c20243 b) Zhang W, Su Z, Yi S, et al. Sandwich structured metal oxide/reduced graphene oxide/metal oxide-based polymer electrolyte enables continuous inorganic-organic interphase for fast lithium-Ion transportation. *Small*. 2023;2207536. doi:10.1002/smll.202207536 c) Han S, Liu S, Gao J, et al. A novel composite polymer electrolyte containing the lithium-ion conductor Li<sub>3</sub>Zr<sub>2</sub>Si<sub>2</sub>PO<sub>12</sub> synthesized by cationic-exchange method for solid lithium metal batteries. *Electrochim Acta*. 2023;441:141795. doi:10.1016/j.electacta.2022.141795 d) Wang D, Jin B, Ren Y, et al. Bifunctional solid-state copolymer electrolyte with stabilized interphase for high-performance lithium metal battery in a wide temperature range. *ChemSusChem*. 2022;15(16):e202200993. doi:10.1002/cssc.202200993 e) Lee K, Shang Y, Bobrin VA, et al. 3D printing nanostructured solid polymer electrolytes with high modulus and conductivity. *Adv Mater*. 2022;34(42):2204816. doi:10.1002/adma.202204816
20. a) Ihrner N, Johannisson W, Sieland F, Zenkert D, Johansson M. Structural lithium ion battery electrolytes via reaction induced phase-separation. *J Mater Chem A*. 2017;5(48):25652. doi:10.1039/C7TA04684G b) Schneider LM, Ihrner N, Zenkert D, Johansson M. Bicontinuous electrolytes via thermally initiated polymerization for structural lithium ion batteries. *ACS Appl Energy Mater*. 2019;2(6):4362. doi:10.1021/acsaem.9b00563 c) Liu X, Ding G, Zhou X, et al. An interpenetrating network poly(diethylene glycol carbonate)-based polymer electrolyte for solid state lithium batteries. *J Mater Chem A*. 2017;5(22):11124. doi:10.1039/C7TA02423A d) Willgert M, Leijonmarck S, Lindbergh G, Malmström E, Johansson M. Cellulose nanofibril reinforced composite electrolytes for lithium ion battery applications. *J Mater Chem A*. 2014;2(33):13556. doi:10.1039/C4TA01139B
21. Chen J, Zhou Y, Islam MS, et al. Carbon fiber reinforced Zn-MnO<sub>2</sub> structural composite batteries. *Compos Sci Technol*. 2021;209:108787. doi:10.1016/j.compscitech.2021.108787
22. Liu X, Han Q, Wang J, Shi M, Liu C. Tree root-inspired structural electrolyte for laminated carbon fiber reinforced composites with high energy density and mechanically-robust properties. *Chem Eng J*. 2022;449:137828. doi:10.1016/j.cej.2022.137828
23. Weber R, Genovese M, Louli AJ, et al. Long cycle life and dendrite-free lithium morphology in anode-free lithium pouch cells enabled by a dual-salt liquid electrolyte. *Nat Energy*. 2019;4(8):683-689. doi:10.1038/s41560-019-0428-9
24. Zhou D, Shanmukaraj D, Tkacheva A, Armand M, Wang G. Polymer electrolytes for lithium-based batteries: advances and

- prospects. *Chem.* 2019;5(9):2326-2352. doi:[10.1016/j.chempr.2019.05.009](https://doi.org/10.1016/j.chempr.2019.05.009)
25. Kovalenko I, Zdyrko B, Magasinski A, et al. A major constituent of Brown algae for use in high-capacity Li-ion batteries. *Science.* 2011;334(6052):75-79. doi:[10.1126/science.1209150](https://doi.org/10.1126/science.1209150)
26. Singer G, Sinn G, Rennhofer H, et al. High performance functional composites by in-situ orientation of carbon nanofillers. *Compos Struct.* 2019;215:178-184. doi:[10.1016/j.compstruct.2019.02.020](https://doi.org/10.1016/j.compstruct.2019.02.020)
27. Carlstedt D, Asp LE. Performance analysis framework for structural battery composites in electric vehicles. *Compos Part B Eng.* 2020;186:107822. doi:[10.1016/j.compositesb.2020.107822](https://doi.org/10.1016/j.compositesb.2020.107822)

## SUPPORTING INFORMATION

Additional supporting information can be found online in the Supporting Information section at the end of this article.

**How to cite this article:** Singer G, Hsieh C-T, Jin T, Lee SH, Yang Y. A quasi-solid polymer electrolyte-based structural battery with high mechanical and electrochemical performance. *EcoMat.* 2023;e12418. doi:[10.1002/eom2.12418](https://doi.org/10.1002/eom2.12418)